JOURNAL OF GEOPHYSICAL RESEARCH, VOL. 112, D01203, doi:10.1029/2006JD007056, 2007

Oxygenated and water-soluble organic aerosols in Tokyo

Y. Kondo,[1] Y. Miyazaki,[1] N. Takegawa,[1] T. Miyakawa,[1] R. J. Weber,[2] J. L. Jimenez,[3] Q. Zhang,[4] and D. R. Worsnop[5]

Received 6 January 2006; revised 9 May 2006; accepted 12 July 2006; published 12 January 2007.

[1] Submicron organic aerosol was measured simultaneously with an Aerodyne aerosol mass spectrometer (AMS) and a particle-into-liquid sampler (PILS) capable of measuring water-soluble organic carbon (WSOC) during the winter and summer of 2004 in Tokyo. Both techniques are being used to investigate the formation of secondary organic aerosol (SOA), and the combined data sets provide unique insights. In summer, about 80% (40–65%) of organic aerosols were oxygenated when scaled by total (carbon) mass concentration, due to high photochemical activity, leading to the active formation of SOA. In winter the fraction of oxygenated organic aerosol is reduced to 39% (total mass base) and 23% (carbon mass base). Previous AMS studies have shown that signals at *m*/*z* 44 of the AMS mass spectra of ambient aerosols are dominated by COO^+, which typically originates from oxygenated organic aerosols (OOA). The signals at *m*/*z* 44 and the derived OOA mass concentrations were highly correlated with WSOC (r^2 = 0.78–0.91) throughout these seasons, indicating that OOA and WSOC were very similar in their chemical characteristics. Approximately 88 ± 29% of OOA was found to be water soluble on the basis of the comparison of the WSOC concentrations with those of oxygenated organic carbon (OOC) derived from the AMS data.

Citation: Kondo, Y., Y. Miyazaki, N. Takegawa, T. Miyakawa, R. J. Weber, J. L. Jimenez, Q. Zhang, and D. R. Worsnop (2007), Oxygenated and water-soluble organic aerosols in Tokyo, *J. Geophys. Res.*, *112*, D01203, doi:10.1029/2006JD007056.

1. Introduction

[2] In many locations, organic aerosols (OA) are a major component of total submicron aerosol mass. In Tokyo, the organic fraction varies between 40 and 60% throughout all seasons [*Takegawa et al.*, 2006]. In the absence of biomass burning emissions, oxygenated organic aerosols (OOA) are thought to be mainly formed by photooxidation of volatile organic compounds (VOCs) followed by condensation on preexisting particles or through homogeneous nucleation [*Odum et al.*, 1996; *Bonn and Moortgat*, 2003]. Some compounds, such as organic acids may also be formed through reactions in cloud droplets [*Warneck*, 2003; *Ervens et al.*, 2004; *Lim et al.*, 2005]. These organic compounds contain various functional groups [e.g., *Saxena and Hildemann*, 1996]. Some organic compounds are hygroscopic and can act as cloud condensation nuclei (CCN) and may play an important role in direct/indirect radiative effects [*Facchini et al.*, 1999; *Jacobson et al.*, 2000].

[3] OA have been quantitatively measured by the Aerodyne aerosol mass spectrometer (AMS) at various locations [*Alfarra et al.*, 2004; *Zhang et al.*, 2005a, 2005c; *Takegawa et al.*, 2005, 2006]. A new algorithm has been developed to quantify OOA and hydrocarbon-like organic aerosol (HOA) separately from AMS mass spectral time series on the basis of a custom principal component analysis [*Zhang et al.*, 2005b, 2005c]. OA observed by the AMS in Tokyo has also been classified approximately into primary organic aerosol (POA) and secondary organic aerosol (SOA) on the basis of a new method of time series analysis, conceptually similar to the EC-OC tracer method [*Takegawa et al.*, 2006]. In their studies, POA and SOA were separated by using the correlation with carbon monoxide (CO) with OA and fragments of aliphatic (*m*/*z* 57) and oxygenated (*m*/*z* 44) organic compounds of the AMS mass spectra. A major portion of POA in Tokyo, defined as the OA components highly correlated with CO, is very likely emitted from vehicles. The SOA, defined as the excess OA (difference between total OA and estimated POA), is assumed to be produced from oxidation of VOCs. The concentrations of POA and SOA agreed well with those of HOA and OOA, respectively, indicating that HOA and OOA are very similar to POA and SOA, at least in Tokyo for the time periods analyzed by *Takegawa et al.* [2006].

[4] On the other hand, a new technique for the continuous measurement of the water-soluble organic carbon (WSOC) fraction of OA has been developed by combining the particle-into-liquid sampler (PILS) with a total carbon (TOC) analyzer (PILS-WSOC) [*Weber et al.*, 2001; *Sullivan et al.*, 2004]. Hydrophilic and hydrophobic fractions of

[1] Research Center for Advanced Science and Technology, University of Tokyo, Tokyo, Japan.
[2] School of Earth and Atmospheric Sciences, Georgia Institute of Technology, Atlanta, Georgia, USA.
[3] Department of Chemistry and CIRES, University of Colorado, Boulder, Colorado, USA.
[4] Atmospheric Science Research Center, University at Albany, SUNY, Albany, New York, USA.
[5] Aerodyne Research, Incorporated, Billerica, Massachusetts, USA.

0148-0227/07/2006JD007056$09.00

Table 1. Summary of the Terminology Used to Describe the Organic Aerosols (OA) in This Study

Terminology	Definition
OA	Organic aerosol, which is approximately equal to OOA + HOA
OM	Organic matter, which is identical to OA
m/*z* 44	Equivalent mass concentration of OA represented by *m*/*z* 44[a]
POA	Primary organic aerosol, OA component linearly correlated with CO[b]
SOA	Secondary organic aerosol = OA − POA − background OA[b]
OOA	Oxygenated OA obtained from AMS mass spectra[a]
HOA	Hydrocarbon-like OA obtained from AMS mass spectra[a]
OOC	Total carbon of OOA obtained from AMS mass spectra[c]
HOC	Total carbon of HOA obtained from AMS mass spectra[c]
OC_{Sunset}	Total carbon of OA measured by thermal optical technique
WSOC	Total carbon of OA that is water soluble collected by PILS-WSOC[d]
WIOC	Total carbon of OA that is water insoluble not collected by PILS-WSOC[b,d]; WIOC = OC_{Sunset} − WSOC
Org.-eq.	Organic equivalent mass concentration of an AMS *m*/*z*[a]

[a] *Zhang et al.* [2005b].
[b] *Takegawa et al.* [2006].
[c] *Zhang et al.* [2005c].
[d] *Sullivan et al.* [2004].

WSOC have been isolated and quantified with this method and used to investigate sources of WSOC at urban sites [*Sullivan and Weber*, 2006]. It is anticipated that organic compounds forming OOA and WSOC are similar because OOA are likely in general to be water soluble or partially soluble in water. Similarly, HOA are likely water insoluble, although these relationships have not been demonstrated experimentally. Comparisons of OOA and WSOC measured by AMS and PILS-WSOC, respectively, can provide insights into both techniques and into the chemical nature of these aerosols. Measurements for this comparison were conducted in Tokyo in the winter and summer of 2004 within the framework of the Integrated Measurement Program for Aerosol and Oxidant Chemistry in Tokyo (IMPACT) campaigns. In this study we use different terminologies for organic compounds in aerosol particles, including OOA and WSOC, depending on the measurement techniques used and aerosol chemical characteristics. A summary of the definitions is provided in Table 1.

2. Measurements

[5] OA (OOA and HOA) and WSOC concentrations were measured simultaneously near the urban center of Tokyo during two periods in 2004: 26 January to 7 February (13 days in winter), and 1–15 August (15 days in summer). The sampling inlet was located approximately 20 m above ground level and the instruments were located within a building at the Research Center of Advanced Science and Technology (RCAST) campus of the University of Tokyo (35.66°N, 139.66°E) in Japan. RCAST is located about 10 km west of the Tokyo Bay coastline and is near the southeastern edge of the Kanto Plain. The sampling location and meteorological conditions are described in detail elsewhere [*Kondo et al.*, 2006; *Takegawa et al.*, 2006; *Morino et al.*, 2006].

[6] WSOC was measured continuously by an online instrument, as described in detail by *Sullivan et al.* [2004]. It measures WSOC with a PILS sampler by growing particles into large water droplets that are collected onto a plate using an impactor. The collected liquid is filtered and the dissolved organic carbon is quantified online by a Total Organic Carbon analyzer (TOC; Sievers Model 800 Turbo, Boulder, CO) providing continuous 6-min integral measurements with a detection limit of approximately 1 μg C m^{-3} (3σ of baseline noise). WSOC is operationally defined here as the fraction of OA which is collected by PILS, penetrates a 0.5 μm stainless steel mesh filter and liquid transport tubing, and is detected by the TOC analyzer. The inlet for the PILS-WSOC was equipped with a PM_1 (1-μm-diameter cutoff size) cyclone (Model URG-2000-30EHB, URG Incorporated, United States) and activated carbon denuder (Sunset Laboratory, Incorporated, Beaverton, Oregon, United States) in an attempt to remove potential interferences from VOCs. WSOC measurement accuracy, on the basis of known uncertainties, is estimated to be between ±5 and 10% [*Sullivan et al.*, 2004]. The estimated accuracies of the measurements of organic aerosols used for quantitative analysis in the present study are summarized in Table 2. The PILS-WSOC measurements made between 4 and 15 August were compared with WSOC manually extracted from 12-hour integrated PM_1 quartz filter (Filter-WSOC). The PILS- and Filter-WSOC measurements ranged between 1–5 μg m^{-3} and agreed to within 12%, indicating that PILS-WSOC measurement is almost identical to the filter based WSOC data [*Miyazaki et al.*, 2006].

[7] In addition to WSOC, total organic carbon (OC) and elemental carbon (EC) of the ambient PM_1 aerosol was measured every 1 hour with an EC-OC analyzer using a thermal optical technique (Sunset Laboratory, Incorporated). The inlet for this instrument was also equipped with a PM_1

Table 2. Accuracies of the Measurements of Organic Aerosols for Typical Mass Concentrations

Compounds	Accuracies, %
OA	±25
OOA	±25
HOA	±25
OOC	±31
HOC	±31
OC_{Sunset}	±16
WSOC	±10
WIOC	±26

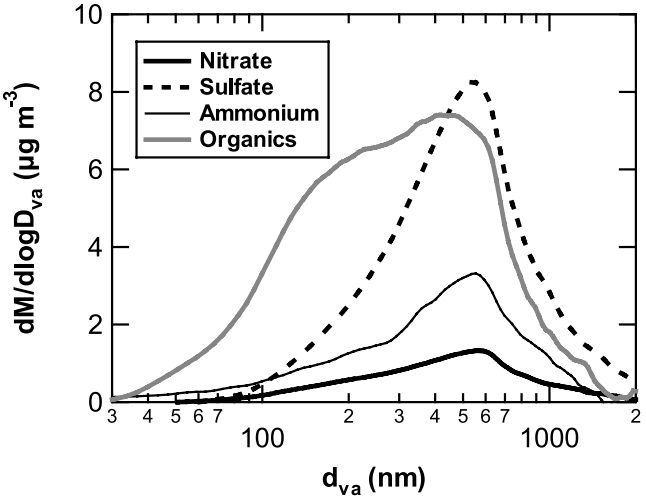

Figure 1a. Average mass size distributions of nitrate (bold line), sulfate (dashed line), ammonium (thin line), and organics (gray line) for the summer of 2004. The horizontal axis is the vacuum aerodynamic diameter (d_{va}).

cyclone and activated carbon denuder. Detailed descriptions of this measurement are given elsewhere [*Kondo et al.*, 2006; *Takegawa et al.*, 2006; *Miyazaki et al.*, 2006]. The overall estimated accuracy and the detection limit (3σ) of the OC measurement (OC_{Sunset}) were 16% and 1 μg m^{-3}, respectively, for the study period [*Takegawa et al.*, 2005]. Water-insoluble organic carbon (WIOC) was defined as OC_{Sunset} − WSOC. Accuracy and detection limit of WIOC, estimated from the errors of these quantities for OC_{Sunset} and WSOC, are 26% and 1.4 μg m^{-3}, respectively.

[8] Mass spectra of OA and total OA concentration were measured every 10 min by the AMS with a detection limit of 0.3 μg m^{-3} for 1 hour averaged data (3σ) [*Takegawa et al.*, 2005]. The inlet for AMS was equipped with a $PM_{2.5}$ cyclone. The AMS aerodynamic lens transmits aerosol particles with diameters smaller than approximately 1 μm. The mass size distributions of non refractory (NR) aerosol (inorganic and organic compounds), *m*/*z* 43, *m*/*z* 44, and *m*/*z* 57 measured by AMS during the summer of 2004 are shown in Figures 1a and 1b. These size distributions are essentially similar to those measured in other observational periods in 2003–2004 [*Takegawa et al.*, 2006]. These size distributions suggest that the NR aerosols measured with the AMS cover the PM_1 size range. The OA mass concentrations were dominated by particles with diameters smaller than 1 μm, considering that the ratio of OC_{Sunset} measured with a PM_1 cyclone to that of $PM_{2.5}$ was 0.73 for September 2003. Comparison of inorganic aerosols (sulfate, nitrate, ammonium, and chloride) measured by AMS and PILS-IC (ion chromatography) [*Weber et al.*, 2001; *Orsini et al.*, 2003] has shown agreement to within 25% or better [*Takegawa et al.*, 2005]. The effect of subtle differences in the size cuts for AMS and PILS should be within the overall difference of ε_{total} = 25%, considering the similarity of the size distribution of these inorganic and organic aerosols in the submicron mode shown in Figures 1a and 1b and by *Takegawa et al.* [2006]. Accuracy in the measurements of inorganic aerosol by AMS (ε_{AMS} (inorg)) can be expressed using those by PILS-IC (ε_{PILS} = 20%, *Takegawa et al.* [2005]), as

$$(\varepsilon_{total})^2 = (\varepsilon_{AMS}(\text{inorg}))^2 + (\varepsilon_{PILS})^2 \quad (1)$$

From equation (1), ε_{AMS} (inorg) is derived to be 15%. The accuracy for organic aerosols by AMS can be estimated to some extent from ε_{AMS} (inorg) and by comparison with the mass concentrations measured by a Tapered Element Oscillating Microbalance (TEOM; Rupprecht and Patashnick Co., Albany, NY) instrument operated at 30°C [*Patashnick and Rupprecht*, 1991]. The inlet for the TEOM instrument was also equipped with a PM_1 cyclone and therefore the mass concentrations measured by TEOM represent those for PM_1 mass concentrations (TEOM-PM_1). Total mass concentration of PM_1 was estimated by summing up the mass concentrations of NR aerosols measured by AMS (NR-PM_1) and EC measured by the EC-OC analyzer (EC_{Sunset}). The EC mass constituted only about 5–10% of the total PM_1 mass throughout the seasons. Figure 2 shows comparison of the sum of PM_1 (Σ PM_1 = NR-PM_1 (inorganic + organic) + EC_{Sunset}) concentrations versus TEOM-PM_1 for the summer of 2004. They are tightly correlated (r^2 = 0.91) and the relationship is expressed as

$$\Sigma PM_1 = 0.91 \times \text{TEOM} - PM_1 - 0.38\left[\mu g\, m^{-3}\right] \quad (2)$$

[9] It should be noted that refractory aerosol other than EC_{Sunset}, including some amounts of sea salt, dust, and metal particles, may also contribute to refractory aerosol mass concentrations. However, diameters of these particles are generally larger than 1 μm [e.g., *Seinfeld and Pandis*, 1998, and references therein] and therefore should not significantly contribute to the TEOM-PM_1. In fact, PM_1 sea salt concentrations have been found to be very small [*Takegawa et al.*, 2005]. More quantitatively, *Kondo et al.* [2006] have shown that EC_{Sunset} agreed quite well with the refractory PM_1 mass concentration, estimated from the

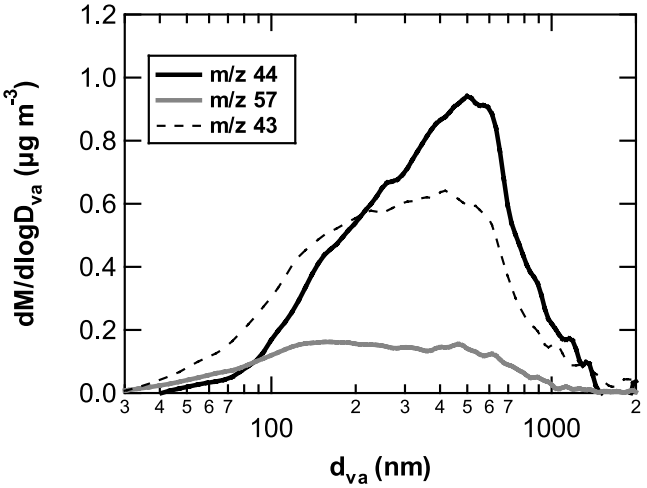

Figure 1b. Same as Figure 1a, but for the average size distributions of *m*/*z* 43 (dashed line), *m*/*z* 44 (bold line), and *m*/*z* 57 (gray line).

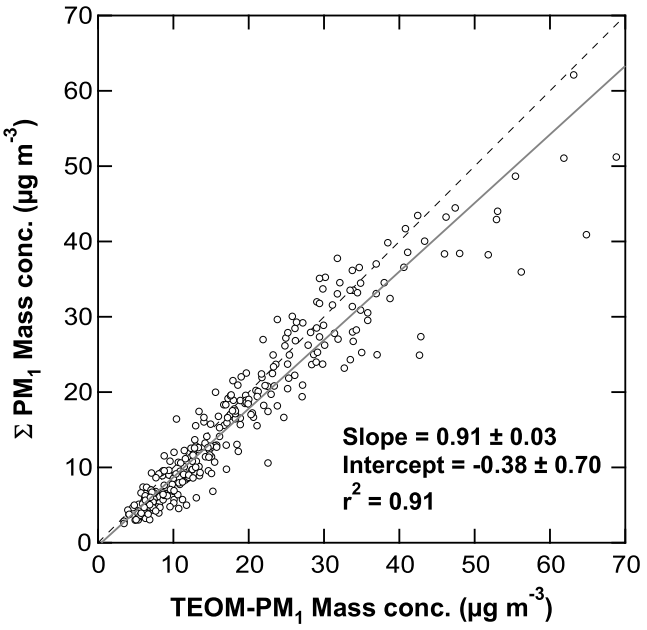

Figure 2. Comparison of mass concentrations of NR-PM_1 + EC_{Sunset} and TEOM-PM_1 for the summer of 2004. Errors represent 2σ.

simultaneously measured size distributions of refractory aerosol for the summer of 2004, namely,

$$\text{Refractory } PM_1 = 0.96 \times EC_{Sunset} - 0.12\left[\mu g\ m^{-3}\right] \quad \left(r^2 = 0.88\right) \tag{3}$$

It should be noted that organic aerosols constituted about 50% of NR-PM_1, as discussed in section 3.1. The good agreement of the NR-PM_1 with TEOM-PM_1 suggests that the accuracy of the AMS organic measurements was comparable to ε_{AMS} (inorg) = 15%. However, we have adopted a conservative value of ε_{total} = 25%, as the accuracy of the AMS organic measurements for the present study.

[10] It should also be noted that the uncertainty in the slope of the relationship given by equation (2) (~4% of the slope) is only that associated with the determination of the regression line (2σ). It does not represent the accuracy of the slope, which is determined mostly by the accuracies of the two variables (Σ PM_1 and TEOM-PM_1 in this case). This error estimate applies to all the slopes of correlations between different variables discussed in this paper. The accuracies in the slopes are noted in the text and are summarized in Table 2.

[11] In addition to WSOC, OA, and OC_{Sunset}, nitrogen oxides (NO_x = NO + NO_2) and total reactive nitrogen (NO_y) were measured using a NO-O_3 chemiluminescence detector combined with a photolytic converter and a gold tube catalytic converter [*Kondo et al.*, 1997; *Takegawa et al.*, 2006].

[12] Previous AMS studies have shown that signals at *m*/*z* 44 of ambient aerosols are dominated by COO^+, which typically originates from oxygenated organics, such as mono/dicarboxylic acids and other oxygenated organic species [*Alfarra*, 2004; *Zhang et al.*, 2005b, and references therein]. On the other hand, *m*/*z* 57 signals in urban areas are typically dominated by aliphatic organic compounds (mostly $C_4H_9^+$). OOA was derived from the recorded AMS mass spectra using the deconvolution algorithm to quantify HOA and OOA separately [*Zhang et al.*, 2005b]. These authors developed two algorithms: algorithm 1, which derives HOA and OOA by a least squares fit in which each *m*/*z* in the organic mass spectrum matrix is expressed as a linear combination of *m*/*z* 44 and *m*/*z* 57, and algorithm 2, which is an iterative procedure expanded from algorithm 1 (also known as "alternating regression" in the factor analysis literature) in which alternating linear regressions are conducted for the time series of all *m*/*z*'s, and then to the whole spectrum at every time step, to improve fitting to the observed OA, commonly referred to also as organic matter (OM). We have used the results from algorithm 2 for the present analysis. Note that in the results of algorithm 2, HOA and OOA are no longer just proportional to *m*/*z* 57 and 44, respectively, since the whole data matrix is used iteratively in the solution procedure.

3. Results and Discussion

3.1. Temporal Variations of OOA, HOA, and WSOC

[13] Time series plots of OOA, HOA, and WSOC for winter and summer are shown in Figure 3. The r^2 values for the correlation between the reconstructed OA (= HOA + OOA) and measured OA are 0.999, indicating that the variance of the total OA mass is almost entirely captured by these two components. Generally in Tokyo, the OA concentrations are strongly controlled by emissions, local production, and regional transport. HOA and OOA are estimated to be produced mainly by combustion and oxidation of VOCs, respectively as discussed by *Takegawa et al.* [2006] and *Zhang et al.* [2005c]. Takegawa et al. studied seasonal and diurnal variations of OA at RCAST in detail using the data obtained by AMS in winter, fall, and summer 2003 and winter 2004, although the summer 2004 data are not included in their studies. Important findings relevant to the present paper are summarized below. The median mass concentrations PM_1-OA were 6–7 $\mu g\ m^{-3}$ throughout the seasons and constituted 40–60% of the total of NR-PM_1 mass loading (12–15 $\mu g\ m^{-3}$). POA and SOA were separated using the method described in section 1. POA correlated well (r^2 = 0.76–0.85) with HOA with slopes ranging from 0.88–1.36 for the winter, summer, and fall periods with no systematic seasonal variations. Correspondingly, SOA also correlated well (r^2 = 0.65–0.85) with OOA with slopes ranging from 0.97–1.41 for the same periods. These results suggest that POA and SOA are similar to HOA and OOA, respectively, in Tokyo. On average, POA did not show a distinct diurnal variation, while SOA showed a clear diurnal pattern reaching peak values in the early afternoon throughout the seasons. The peak SOA values were comparable to those for POA, suggesting photochemical SOA formation in daytime. A second peak in SOA was also found to occur at around 21:00 local time, suggesting additional formation of SOA after sunset.

[14] The WSOC concentrations measured in winter, summer, and fall 2004 have been found to correlate well with SOA (r^2 = 0.70–0.79), and to show seasonal and diurnal variations similar to those for SOA [*Miyazaki et al.*, 2006].

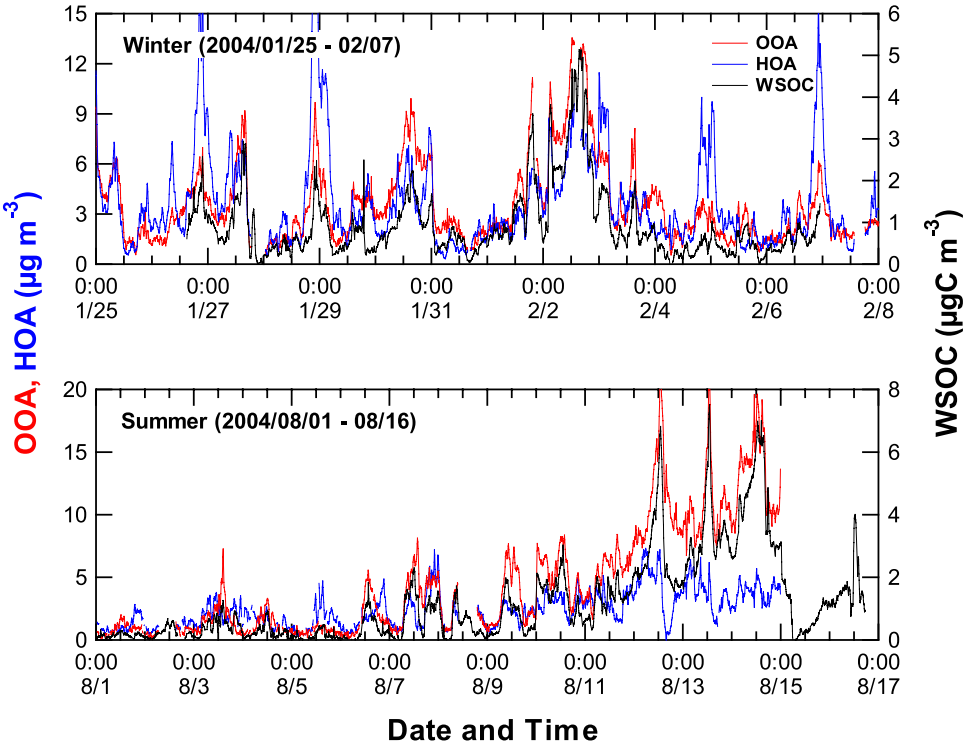

Figure 3. Time series plots of oxygenated organic aerosol (OOA), hydrocarbon-like aerosol (HOA), and water-soluble organic carbon (WSOC) observed in Tokyo in January–February and August 2004.

The median WSOC/OC_{Sunset} ratios peaked in the early afternoon and the median ratios for the whole observational periods were 0.19, 0.35, and 0.35 μgC/μgC for the winter, summer, and fall of 2004, respectively. The maximum WSOC/OC_{Sunset} ratios were 0.37 and 0.86 μgC/μgC for winter and summer, respectively, suggesting that air masses sampled in summer and fall were more photochemically processed than those in winter. In fact, in summer, OOA (WSOC) was significantly elevated over HOA on sunny days, especially between 12–14 August (Figure 3). On these days, air stagnated in Tokyo from the morning to early afternoon and ozone concentrations exceeded 100 ppbv in correlation with the elevated levels of OOA in the early afternoon. The correlated variations between OOA and WSOC are immediately seen in Figure 3.

[15] The seasonal variation of the formation of OOA and WSOC, discussed above, is also clearly seen from their correlations with OA (from the AMS) and OC_{Sunset} shown in Figures 4a and 4b, respectively. OOA correlated tightly (r^2 = 0.89) with OA in the summer with a slope of 0.81 μg/μg, indicating that dominant fraction of the OA mass concentration was in the form of OOA. WSOC also correlated tightly (r^2 = 0.85) with OC_{Sunset}, consistent with the similarity between OOA and WSOC, discussed in detail in sections 3.3 and 3.4. However, it should be noted that the slope of the WSOC-OC_{Sunset} correlation is 0.42μgC/μgC, about half of that for OOA-OA. This difference is due to the about factor of two larger OOA/OOC (oxygenated organic carbon = total carbon concentration ratios in OOA) ratio than the HOA/HOC (hydrocarbon-like organic carbon = total carbon concentration ratios in HOA). The OOA/OOC and HOA/HOC ratios are discussed in more detail in section 3.4. In this study we derive ratios among different oxygenated organics, including OA, OC_{Sunset}, WSOC, OOA, HOA, OOC, and HOC. They are summarized in Table 3.

[16] For winter, the average slope of the OOA-OA correlation is 0.39 μg/μg, which is about half of that for summer. More importantly, it should be noted that the OOA-OA correlation split into two major branches (high OOA/OA and low OOA/OA). The slope of the high OOA/OA branch (about 0.60 μg/μg) is about 75% of that for the summer OOA-OA correlation. The slope of the OOA/OA branch was as low as about 0.25 μg/μg. These features are not clearly seen in the WSOC- OC_{Sunset} correlation (Figure 4b), partly due to a smaller number of the data points. The high OOA/OA data

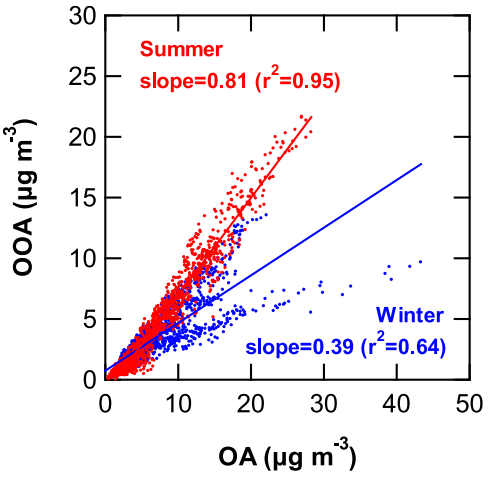

Figure 4a. OOA-OA correlations for winter and summer.

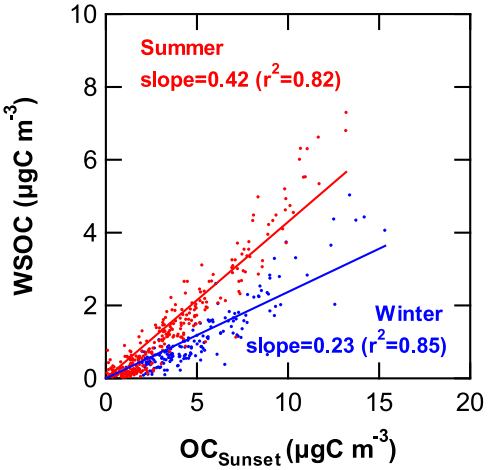

Figure 4b. WSOC-OC_{Sunset} correlations for winter and summer.

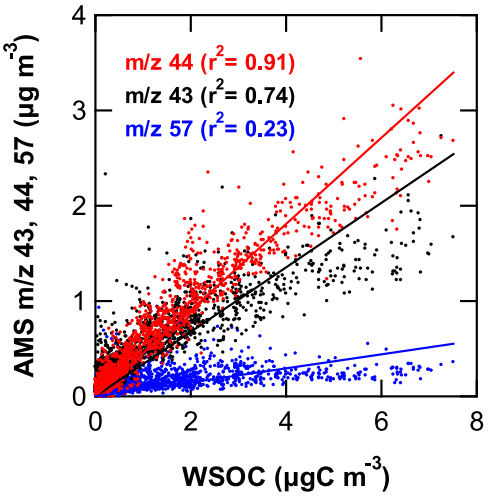

Figure 5. Correlations of AMS *m/z* 44, *m/z* 43, and *m/z* 57 with WSOC for summer.

were taken mostly on 2 February, when OOA (and OA) reached its highest concentrations during this period. On this day, the sampling site (RCAST) was located behind a surface cold front associated with a low-pressure system, developing just south of the Japanese mainland. Significant precipitation occurred and the local surface wind was northerly during the whole day, transporting pollutants from inland of the Kanto Plain. It is likely that these air masses were moderately aged. On the other hand, the data with the low OOA/OA ratios (high HOA/OOA ratios) were taken mostly around midnight of 27 and 29 January and 5 and 7 February, when HOA was very high (Figure 3). During these periods, HOA emitted from vehicles accumulated under very calm conditions. HOA and EC_{Sunset} concentrations generally tended to increase with decreasing wind speeds (not shown) [*Kondo et al.*, 2006; *Takegawa et al.*, 2006]. The low boundary layer height during the nighttime also contributed to the high levels of HOA. The low OOA/OA branch represents the correlation for organic aerosols, strongly influenced by fresh emissions from vehicles. The similarity of the OOA-OA slope of the high OOA/OA branch for winter to that for summer may suggest active formation of OOA even in winter, consistent with the analysis by *Takegawa et al.* [2006].

Table 3. Average Ratios (Slopes) Among OA, OC_{Sunset}, WSOC, WIOC, OOA, HOA, OOA, and OOC in Units of $\mu g/\mu g$ (e.g., OOA/OA), $\mu g/\mu gC$ (e.g., OOA/WSOC), or $\mu gC/\mu gC$ (e.g., OOC/WSOC)[a]

Ratios	Winter	Summer
Ratios for Compounds Similar in Chemical Characteristics		
OOA/WSOC	3.31 ± 0.06 (0.86)	3.16 ± 0.04 (0.93)
HOA/WIOC	1.26 ± 0.19 (0.52)	1.14 ± 0.07 (0.59)
OOA/OOC	2.40	2.27
HOA/HOC	1.16	1.16
OOC/WSOC (uncorrected)	1.41 ± 0.03 (0.86)	1.29 ± 0.02 (0.93)
OOC/WSOC (corrected)	1.23 ± 0.03 (0.86)	1.06 ± 0.02 (0.93)
HOC/WIOC	1.07 ± 0.16 (0.52)	0.94 ± 0.06 (0.59)
OC_{AMS}/OC_{Sunset}	1.14 ± 0.08 (0.72)	1.21 ± 0.03 (0.87)
Ratios for Other Combinations		
OOA/OA	0.39 ± 0.01 (0.64)	0.81 ± 0.01(0.89)
HOA/OA	0.62 ± 0.01 (0.89)	0.20 ± 0.01(0.60)
OA/OC_{Sunset}	1.72 ± 0.01 (0.80)	2.22 ± 0.05 (0.89)
$WSOC/OC_{Sunset}$	0.23 ± 0.04 (0.82)	0.42 ± 0.0.03 (0.85)
HOA/WSOC	7.72 ± 0.19 (0.28)	0.96 ± 0.04 (0.39)
OOC/OC_{Sunset}	0.23 ± 0.01 (0.58)	0.65 ± 0.01 (0.89)
HOC/OC_{Sunset}	0.79 ± 0.01 (0.94)	0.39 ± 0.01 (0.74)
HOA/OOA	1.71 ± 0.06 (0.35)	0.21 ± 0.01 (0.39)

[a]The errors represent 2σ, and numbers in the brackets are r^2 values for the correlations.

3.2. AMS Mass Spectra

[17] The AMS *m/z* 44 and WSOC showed similar temporal variations both in winter and summer, while *m/z* 57 behaved differently (not shown). This can be seen in the scatter plots of *m/z* 44, *m/z* 43, and *m/z* 57 versus WSOC shown in Figure 5 for summer. The scatter plots of *m/z* 44 versus WSOC for winter and summer are compared in Figure 6. The slopes, their uncertainties (2σ), and r^2 for winter and summer are summarized in Table 4. The peak at *m/z* 43 is typically a mixture of several ions, including aliphatic ($C_3H_7^+$) and oxygenated ($C_2H_3O^+$) fragments [*Zhang et al.*, 2005b, and references therein; *DeCarlo et*

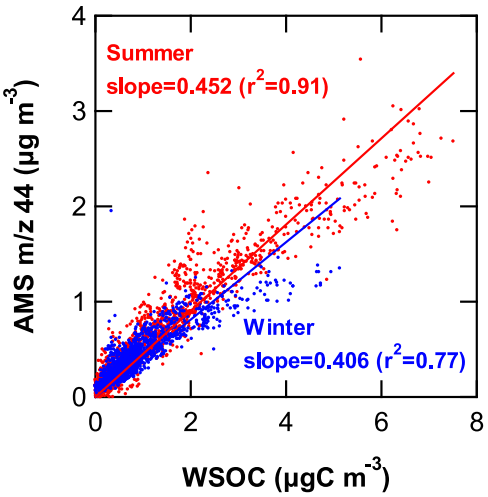

Figure 6. Correlations of AMS *m/z* 44 with WSOC for winter and summer.

Table 4. Correlations of the AMS Organic Equivalent Mass Concentrations (*m/z* 43, 44, and 57) With the WSOC Concentrations

m/z	Slope[a]	Uncertainty[b]	r^2
	Winter		
43	0.592	0.017	0.43
44	0.406	0.009	0.77
57	0.254	0.010	0.23
	Summer		
43	0.338	0.007	0.74
44	0.439	0.006	0.91
57	0.074	0.003	0.23

[a]The slope is in the units of org.-equation $\mu g/\mu gC$.

al., 2006]. Correlation was very tight for *m/z* 44 (r^2 = 0.77–0.91), moderately tight for *m/z* 43 (r^2 = 0.43–0.74), and poor for *m/z* 57 (r^2 = 0.23). Highest correlation of *m/z* 44, a representative tracer of OOA, strongly suggests that organic compounds constituting OOA and WSOC are likely similar compounds in the ambient aerosol. The poor correlation of *m/z* 57 suggests that HOA compounds contribute little to WSOC. This point is discussed in a more quantitative way in section 3.4. The intermediate correlation of *m/z* 43 is consistent with previous studies, which show that *m/z* 43 signal has contributions from both OOA and HOA, as discussed above. Generally, in urban air, *m/z* 43 signals show bimodal size distributions, while *m/z* 44 is mostly in the accumulation mode and likely from species internally mixed with inorganic aerosols, as shown in Figures 1a and 1b and by other studies [e.g., *Takegawa et al.*, 2006; *Zhang et al.*, 2005a]. In this way, the differences in the degree of correlation of the typical AMS spectral markers with WSOC are consistent with anticipated organic compounds measured with AMS and PILS-WSOC. The slopes of the *m/z* 44-WSOC correlation were 0.406 ± 0.006 (2σ) and 0.439 ± 0.003 (2σ) org.-equivalent $\mu g/\mu gC$, for winter and summer, respectively, showing a small seasonal variability of ±0.016 (±4%) org.-equivalent $\mu g/\mu gC$, although the maximum concentrations of *m/z* 44 were higher for summer than winter by a factor of about 2–3. The summer high values were due to higher photochemical activity, as discussed above.

3.3. OOA-WSOC Correlation

[18] The correlation between OOA and WSOC is further investigated in this section to understand their similarities more quantitatively. OOA is plotted versus WSOC for different seasons in Figure 7a. These plots are color coded by the NO_x/NO_y ratio, with lower ratios serving as an indicator of greater air mass photochemical processing. Highest OOA and WSOC concentrations occurred when the air was processed. This is more clearly seen in summer when the NO_x/NO_y ratios reached low values of 0.3–0.5. This agrees with the notion that most of the OOA and WSOC is from SOA formation. OOA is tightly correlated (r^2 = 0.86–0.93) with WSOC throughout the seasons, as was *m/z* 44. The correlation coefficients are larger for OOA than *m/z* 44 alone, which indicates that algorithm 2 of *Zhang et al.* [2005b] produces a more robust estimate of OOA by using the information in the whole AMS mass spectrum.

[19] The slope of the OOA-WSOC correlation tends to be somewhat lower at higher WSOC concentrations, where the NO_x/NO_y ratios were lower, especially in summer. The same feature is also seen for the *m/z* 44-WSOC correlation. A possible explanation for this is that as the OOA is more photochemically processed/aged as its concentration builds up, more of it may become water soluble. It is also possible that as the aerosol concentrations increase because of secondary organic and inorganic aerosol formation, the size distribution grows past the upper size cut of the AMS aerodynamic lens and OOA is underestimated, although it is difficult to prove this from the observed AMS size distributions. However, it is unlikely that this effect significantly changes the overall OOA-WSOC slope, considering the good agreement of the Σ PM_1 with TEOM-PM_1. The average OOA-WSOC slope for these seasons is 3.24 $\mu g/\mu gC$ with a very small seasonal variability of ±0.08 (±2%) $\mu g/\mu gC$.

[20] For comparison with the OOA-WSOC correlations, the HOA-WSOC and HOA-OOA correlations are shown in Figures 7b and 7c. High HOA and low WSOC concentrations occur at low NO_x/NO_y ratios (unprocessed air), especially in summer, consistent with the notion that HOA is equivalent with POA. For winter, this feature is less clear,

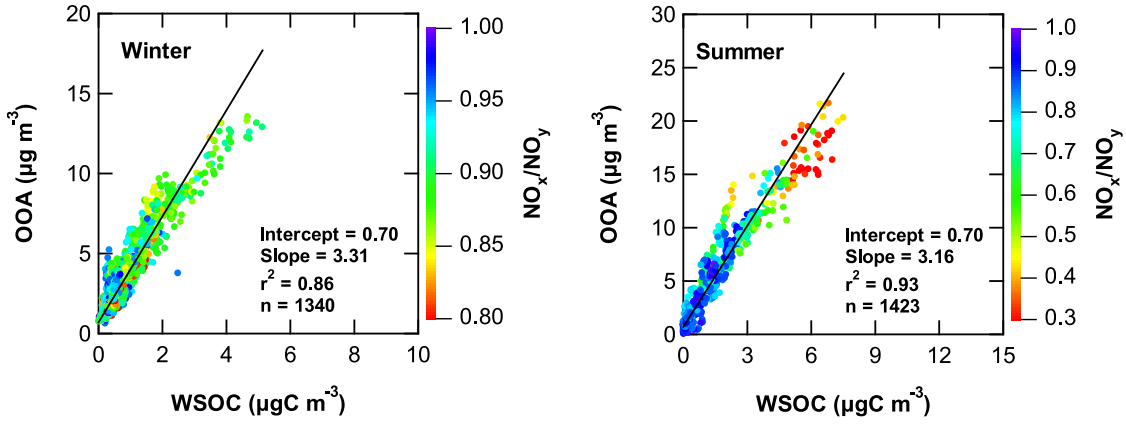

Figure 7a. Correlation of OOA with WSOC for winter and summer. The number of data points is given by *n*. The data points are color coded by the NO_x/NO_y ratios.

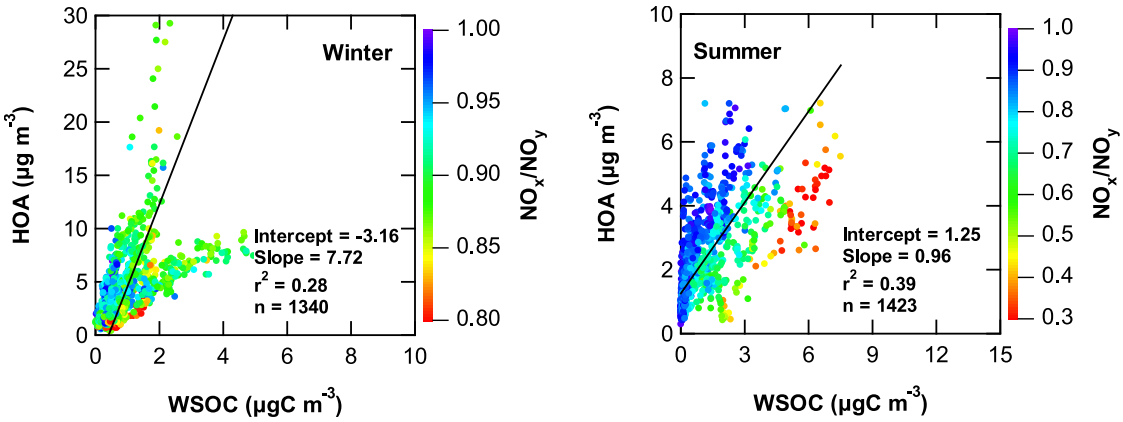

Figure 7b. Correlation of HOA with WSOC for winter and summer.

because of the narrower range of the NO_x/NO_y ratios (0.8–1.0). As anticipated from the *m/z* 57-WSOC and *m/z* 43-WSOC correlations, the HOA-WSOC correlations are much poorer than those for OOA-WSOC. In addition, HOA-OOA and HOA-WSOC correlations are basically similar. It should be noted that for winter HOA-WSOC and HOA-OOA correlations split into two branches. The high HOA/WSOC and HOA/OOA branch corresponds to the low OOA/OA branch, discussed in section 3.1. (Figure 4a). It has been shown that these data were strongly influenced by fresh POA emissions from vehicles. These data constitute low WSOC (<2 μg m^{-3}) regime of the OOA-WSOC correlation (Figure 7a). On the other hand, the low HOA/WSOC (HOA/OOA) branch corresponds to the high OOA/OA branch. It is likely that these organic aerosols were processed, despite the lower photochemical activity in winter.

[21] These results indicate that the correlation between HOA and WSOC, although weak, mainly arises from the correlation between HOA and OOA, which, in turn, is likely due to injection of HOA and formation OOA in same air masses during transport, as discussed in section 3.1. OOA is tightly correlated with WSOC, despite the significant scatter in the HOA-WSOC or HOA-OOA correlations, partly reflecting the variability in chemical aging of air masses. Therefore we conclude that OOA and WSOC are very similar in their chemical characteristics, and that the contribution of HOA to WSOC is small.

3.4. OOA/Oxygenated Organic Carbon (OOC) and OOC/WSOC Ratios

[22] Ratios of OOA to total carbon concentrations in OOA, defined as oxygenated organic carbon (OOC), can provide insight into the molecular composition of OOA because they provide a measure of the average molecular organic mass to organic carbon mass in the aerosol particles. For this purpose, OOC was derived from the OOA mass spectra by the method given by *Zhang et al.* [2005c]. This method assumes an elemental composition (C, H, and O) of each *m/z* in the OOA mass spectra based on knowledge from AMS laboratory experiments and from high-resolution mass spectrometry, and thus allows for the estimation of the elemental composition of OOA. The average OOA/OOC ratios calculated from the derived molar ratio of C:H:O in OOA were 2.40 and 2.27 μg/μgC for winter and summer, respectively. The derived OOA/OOC ratio of 2.34 ± 0.05 (seasonal variability) μg/μgC averaged for winter and summer is similar to that of 2.2 μg/μgC, which was derived for Pittsburgh (September) [*Zhang et al.*, 2005c].

[23] The estimated OOA/OOC ratios can be validated by the OC derived from the AMS data. For this purpose, total

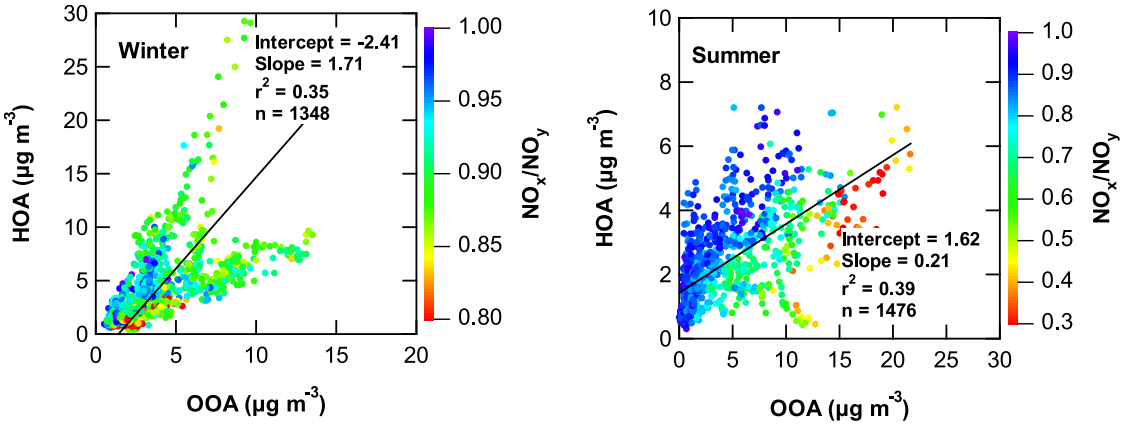

Figure 7c. Correlation of HOA with OOA for winter and summer.

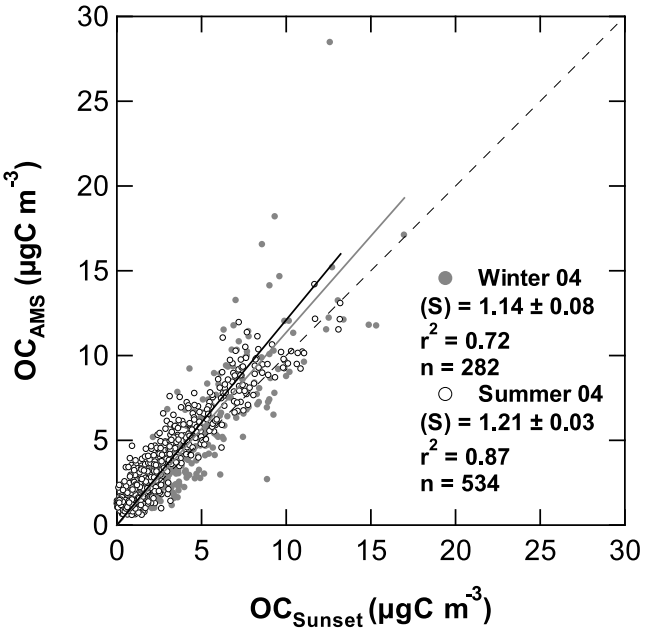

Figure 8. Correlation of OC concentrations derived from the AMS (OC_{AMS}) with those measured by the thermal optical instrument (OC_{Sunset}) for winter and summer. The least squares fitting was derived assuming a zero intercept. Errors represent 2σ.

carbon concentrations in HOA, defined as hydrocarbon-like organic carbon (HOC), were derived by estimating the C:H:O molar ratio in a way similar to that for OOA. The HOA/HOC ratios were estimated to be 1.16 μg/μgC for both winter and summer. Again, this value is close to that of 1.2 μg/μgC, estimated for Pittsburgh [*Zhang et al.*, 2005c]. The OC concentrations derived from the AMS (OC_{AMS} = OOC + HOC) and OC_{Sunset} are compared in Figure 8. The slopes of the least squares fitting of the OC_{AMS} versus OC_{Sunset} scatter plots assuming a zero intercept, are 1.14 and 1.21 for winter and summer, respectively, suggesting that systematic difference of OC obtained by the two methods is within 18%. The accuracy of OOC is determined by the accuracies of OOA and the OOA/OOC ratio. The accuracy of OOA is assumed to be the same for OA, which is ±25%, as discussed in section 2. The accuracy of the OOA/OOC ratio (approximately ±18%) was estimated to be equal to the difference between OC_{AMS} and OC_{Sunset}. The overall accuracy of OOC is estimated to be ±31%.

[24] Classifications of OA into OOA-HOA and water-soluble (WSOC)–water-insoluble (WIOC) organic carbon are not identical in a strict sense, although OOA has already been shown to be similar to WSOC. The former is based on chemical composition (mass spectral patterns, which depend on the initial composition plus fragmentation patterns) and the latter on water solubility at high dilution ratios of the order of 10^7 water/organic mass ratio. An investigation of the relationship between HOA and WIOC should give us further insights on the classification of OA. For this purpose, the derived HOC concentrations are plotted versus those for WIOC (= OC_{Sunset} – WSOC) in Figure 9. The HOC-WIOC correlations have significantly more scatter (r^2 = 0.52–0.58) than the OOA-WSOC correlations (r^2 = 0.86–0.93), as WIOC is the subtraction of two large numbers, each of which contains noise. The HOC/WIOC ratios were 1.07 ± 0.09 and 0.98 ± 0.04, for winter and summer, respectively, suggesting that almost all the HOC was water insoluble and the major portion of WIOC was HOC. The accuracy of the HOC/WIOC ratio is estimated to be about ±40% from the accuracy of HOC (±31%) and WIOC (±26%). From these results, it is likely that almost all WSOC is oxygenated, but not all OOA species are soluble in water, which can be conceptually represented as,

$$\mathrm{OOC} \geq \mathrm{WSOC} \equiv \Sigma(\mathrm{OOC})_i \times f_i \qquad (4)$$

[25] Here, $(OOC)_i$ represents carbon mass concentration of i^{th} OOA species and f_i= 0 or 1) is water solubility in the very dilute solutions in the PILS-WSOC. Equation (4) holds, if the summation is taken for all major $(OOC)_i$ species.

[26] The OOC concentrations, derived from OOA as mentioned above, are plotted versus WSOC concentrations in Figure 10. The OOC-WSOC slopes are derived to be 1.41 and 1.29 μgC/μgC for winter and summer, respectively (uncorrected OOC/WSOC values in Table 3). The accuracy of the OOC/WSOC ratio of 1.35 ± 0.06 (seasonal variability) μgC/μgC is estimated to be about ±33% from the accuracies of OOC and WSOC. Taken at face value, this result means that approximately 74%= 1/1.35) of OOC was water soluble and approximately 26% was insoluble. However, if we recall that OC_{AMS} was larger than OC_{Sunset} by about 1.18 (Figure 8 and associated discussion above) a better estimate is that about 81% and 94% (with an uncertainty of 29%) of the OOC is water soluble in winter and summer, respectively and about 6–19% is water insoluble (corrected OC/WSOC values in Table 3). This result also suggests that in summer, more OOC was water soluble

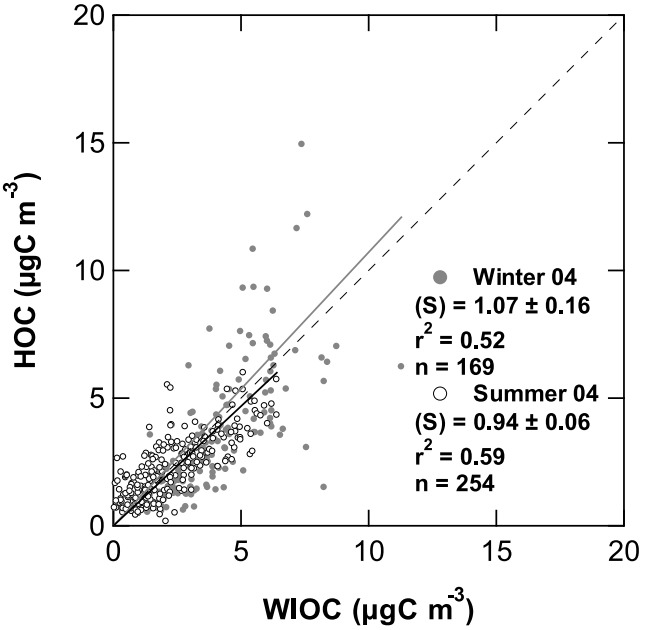

Figure 9. Correlation of concentrations of HOC and WIOC for winter and summer. The least squares fitting was derived assuming a zero intercept. Errors represent 2σ.

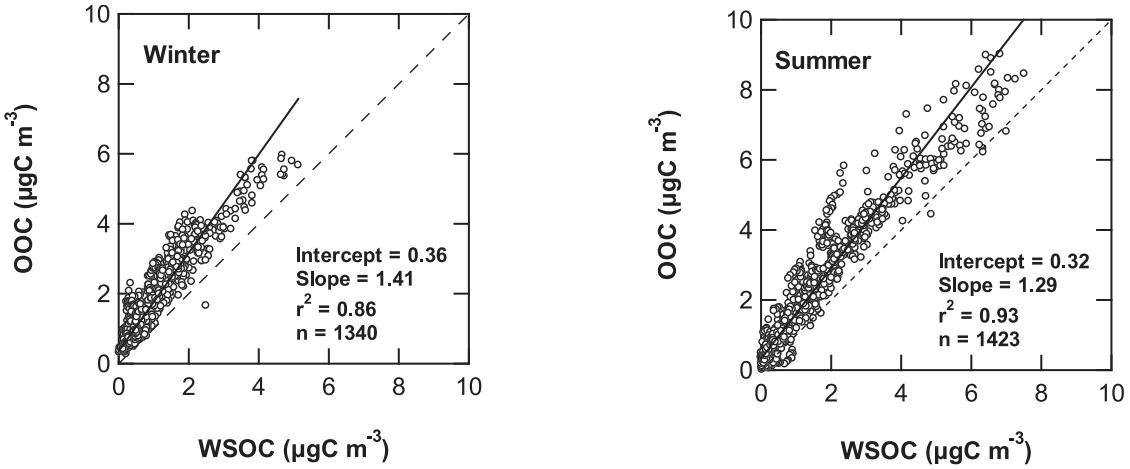

Figure 10. Correlation of OOC with WSOC for winter and summer.

than in winter, although this point is not conclusive because of the combined uncertainties in the measurements.

[27] If about 6–19% of OOC is water insoluble, about 4% and 3% of WIOC must be oxygenated, for winter and summer, respectively, considering that the average WSOC/WIOC and therefore OOC/WIOC ratios were about 0.25 and 0.50. Conversely, the average HOC/WIOC ratios are predicted to be 0.96–0.97, consistent with the derived HOC/WIOC ratio close to 1. Note that for the discussion of the HOC/WIOC ratio, it was not corrected by the factor of $OC_{AMS}/OC_{Sunset} = 1.18$, because of the large uncertainty (40%) in the HOC/WIOC ratio.

3.5. OOA/OA and OOC/OC (WSOC/OC) Ratios

[28] In summer, OOA was highly correlated with OA ($r^2 = 0.89$) and the OOA/OA ratio was as high as 0.81 $\mu g/\mu g$, as discussed in section 3.1. The slope of the OOC-OC_{Sunset} correlation is estimated to be 0.65 $\mu gC/\mu gC$ (Table 3), using the OOC derived in section 3.4. This slope is somewhat higher than the value of 0.42 $\mu gC/\mu gC$ for the WSOC/OC_{Sunset} ratio, due partly to the difference in the OOC and WSOC (section 3.4). For winter, the average OOC/OC_{Sunset} ratio was as low as 0.23 $\mu gC/\mu gC$ ($r^2 = 0.58$), which is very close to the WSOC/OC_{Sunset} ratio ($r^2 = 0.82$). Although the OOA-OA correlation split into the high OOA/OA and low OOA/OA branches, the OOC- OC_{Sunset} correlation did not show clear branching (not shown), similarly to the WSOC- OC_{Sunset} correlation. Considering these results, it should be noted that the ratio of the oxygenated organic aerosol to the total organic aerosol depends on the parameters used to represent organic aerosol concentrations, namely, total mass concentration or carbon mass concentration, in this case. In summer about 80% and 42–65% of organic aerosols were oxygenated when scaled by total mass and carbon mass concentration, respectively. In winter, the degree of oxidation of organic aerosol is reduced to 39% (total mass base) and 23% (carbon mass base).

3.6. Comparison of OOA/OOC with OA/OC

[29] The OOA/OOC ratio of 2.34 ± 0.05 (seasonal variability) $\mu g/\mu gC$ estimated in this study is compared with OA/OC ratios for water-soluble organics from literature, assuming that practically all the OOA was water soluble. The OA/OC ratio ranges between 1.7 and 3.6 $\mu g/\mu gC$ for water-soluble organics that have been measured or are predicted to be present in aerosols [*Turpin and Lim*, 2001; *Saxena and Hildemann*, 1996]. For these studies, water-soluble organics are defined as OA composed of compounds with water solubility of more than 1 g per 100 g of water. Ambient measurement of 13 water-soluble organic species (six diacids, glyoxal, five ketoacids, and one hydrooxy diacid (malic acid)) were conducted in Tokyo on 4 days total in the winter and summer of 1992 [*Sempere and Kawamura*, 1994]. In that study the OA/OC ratio is calculated to be 3.18 ± 0.06 (seasonal variability) $\mu g/\mu gC$ on the basis of the results from those ambient measurements and the molecular weight per carbon weight data [*Turpin and Lim*, 2001]. In that study, the measured compounds accounted for 5–20% of the water-soluble organic mass. The value of 3.18 $\mu g/\mu gC$ agrees with the present OOA/WSOC ratio of 2.92 ± 0.03 $\mu g/\mu gC$ to within 9%. If only 88% of OOA mass is assumed to be water soluble, as observed here, the difference increases to 24%. In any case, this comparison is only qualitative, considering that only very limited portion of the water-soluble organic mass was collected by *Sempere and Kawamura* [1994].

4. Summary and Conclusions

[30] Submicron organic aerosols were measured simultaneously with the Aerodyne aerosol mass spectrometer (AMS), particle-into-liquid sampler (PILS) capable of measuring water-soluble organic carbon (WSOC), and thermal-optical organic carbon (OC) analyzer during the winter and summer of 2004 in Tokyo. Oxygenated organic aerosol (OOA) and hydrocarbon-like organic aerosol (HOA) were quantified separately from AMS mass spectral time series using an algorithm based on a custom principal component analysis. In summer, about 80% (40–65%) of organic aerosols were oxygenated when scaled by total (carbon) mass concentration, due to high photochemical activity, leading to the active formation of SOA. In winter, the degree of oxidation of organic aerosol is reduced to 39% (total mass base) and 23% (carbon mass base), respectively.

[31] Time series of AMS *m*/*z* 44 (*m*/*z* 57), a good marker of OOA (HOA), were highly (poorly) correlated with $r^2 = 0.78–0.91$ ($r^2 = 0.22–0.23$) with WSOC measured with the PILS-WSOC instrument in Tokyo in winter and summer

2004. The *m*/*z* 44-WSOC slope was nearly constant at 0.423 ± 0.016 org.-equation μg/μgC or ±4% (seasonal variability) for winter and summer. The signal at *m*/*z* 44 is an excellent marker for WSOC, considering the high-*m*/*z* 44-WSOC correlation and the stable *m*/*z* 44/WSOC ratio, independent of the season. OOA was even more strongly correlated (r^2 = 0.87–0.93) with WSOC, despite the significant variabilities in the OOA/OC and HOA/OOA (WSOC) ratios, especially in winter. The average OOA/WSOC ratio was 3.24 ± 0.08 μg/μgC or ±2% (seasonal variability). By contrast, HOA was poorly correlated (r^2 = 0.18–0.39) with WSOC and better correlated (r^2 = 0.52–0.58) with water-insoluble organic carbon (WIOC). The high OOA-WSOC correlation, combined with the poor HOA-WSOC correlation, indicates that OOA and WSOC represent a very similar set of species in the aerosol.

[32] The average OOA/oxygenated organic carbon (OOC) ratio was derived to be 2.34 ± 0.05 (seasonal variability) μg/μgC from the OOA mass spectra. OOC was derived from OOA using this ratio. The resulting WSOC/OOC ratios were 0.71 and 0.79 μgC/μgC for winter and summer, respectively. Combined with the observed OC_{AMS}/OC_{Sunset} ratio, these results indicate that about 88 ± 29% of OOA was water soluble for both winter and summer. About 12% of the OOA mass should be water insoluble, and this water-insoluble OOA is estimated to contribute to the 3–4% of the water-insoluble organic mass, considering the WSOC/WIOC ratios.

[33] **Acknowledgments.** This work was supported by the Ministry of Education, Culture, Sports, Science, and Technology (MEXT), the Japanese Science and Technology Agency (JST), and the global environment research fund of the Japanese Ministry of the Environment (C-051). The participation of JLJ and QZ in this study has been supported by NSF grant ATM-0449815 and EPA grant RD-83216101-0. Any opinions, findings, and conclusions or recommendations expressed in this material are those of the authors and do not reflect the views of NSF or EPA.

References

Alfarra, M. R. (2004), Insights into atmospheric organic aerosols using an aerosol mass spectrometer, Ph.D. dissertation, Univ. of Manchester, U. K.

Alfarra, M. R., et al. (2004), Characteristics of urban and rural organic particulate in the Lower Fraser Valley using two Aerodyne aerosol mass spectrometers, *Atmos. Environ.*, *38*, 5745–5758.

Bonn, B., and G. K. Moortgat (2003), Sesquiterpene ozonolysis: Origin of atmospheric new particle formation from biogenic hydrocarbons, *Geophys. Res. Lett.*, *30*(11), 1585, doi:10.1029/2003GL017000.

DeCarlo, P. F., J. R. Kimmel, A. Trimborn, M. J. Northway, J. T. Jayne, A. C. Aiken, M. Gonin, K. Fuhrer, T. Horvath, K. Docherty, D. R. Worsnop, and J. L. Jimenez (2006), Field-deployable, high-resolution, time-of-flight aerosol mass spectrometer, *Anal. Chem.*, *78*(24), 828–8289.

Ervens, B., G. Feingold, G. J. Frost, and S. M. Kreidenweis (2004), A modeling study of aqueous production of dicarboxylic acids: 1. Chemical pathways and speciated organic mass production, *J. Geophys. Res.*, *109*, D15205, doi:10.1029/2003JD004387.

Facchini, M. C., M. Mircea, S. Fuzzi, and R. J. Charlson (1999), Cloud albedo enhancement by surface-active organic solutes in growing droplets, *Nature*, *401*, 257–259.

Jacobson, M. C., H.-C. Hansson, K. J. Noone, and R. J. Charlson (2000), Organic atmospheric aerosols: Review and state of the science, *Rev. Geophys.*, *38*, 267–294.

Kondo, Y., et al. (1997), The performance of an aircraft instrument for the measurement of NO_y, *J. Geophys. Res.*, *102*, 28,663–28,671.

Kondo, Y., et al. (2006), Temporal variations of elemental carbon in Tokyo, *J. Geophys. Res.*, *111*, D12205, doi:10.1029/2005JD006257.

Lim, H. J., A. G. Carlton, and B. J. Turpin (2005), Isoprene forms secondary organic aerosol through cloud processing: Model simulations, *Environ. Sci. Technol.*, *39*, 4441–4446.

Miyazaki, Y., Y. Kondo, N. Takegawa, Y. Komazaki, K. Kawamura, M. Mochida, K. Okuzawa, and R. J. Weber (2006), Time-resolved measurements of water-soluble organic carbon in Tokyo, *J. Geophys. Res.*, *111*, D23206, doi:10.1029/2006JD007125.

Morino, Y., Y. Kondo, N. Takegawa, Y. Miyazaki, K. Kita, Y. Komazaki, M. Fukuda, T. Miyakawa, N. Moteki, and D. R. Worsnop (2006), Partitioning of HNO_3 and particulate nitrate over Tokyo: Effect of vertical mixing, *J. Geophys. Res.*, *111*, D15215, doi:10.1029/2005JD006887.

Odum, J. R., T. Hoffmann, F. Bowman, D. Collins, R. C. Flagan, and J. H. Seinfeld (1996), Gas/particle partitioning and secondary organic aerosol yield, *Environ. Sci. Technol.*, *30*, 2580–2585.

Orsini, D., Y. Ma, A. Sullivan, B. Sierau, K. Baumann, and R. J. Weber (2003), Refinements to the particle-into-liquid sampler (PILS) for ground and airborne measurements of water soluble aerosol composition, *Atmos. Environ.*, *37*, 1243–1259.

Patashnick, H., and E. G. Rupprecht (1991), Continuous PM-10 measurements using the Tapered Element Oscillating Microbalance, *J. Air Waste Manage.*, *41*, 1079–1083.

Saxena, P., and L. Hildemann (1996), Water-soluble organics in atmospheric particles: A critical review of the literature and application of thermodynamics to identify candidate compounds, *J. Atmos. Chem.*, *24*, 7–109.

Seinfeld, J. H., and S. N. Pandis (1998), *Atmospheric Chemistry and Physics*, 1326 pp., John Wiley, Hoboken, N. J.

Sempere, R., and K. Kawamura (1994), Comparative distributions of dicarboxylic acids and related polar compounds in snow, rain and aerosols from urban atmosphere, *Atmos. Environ.*, *28*, 449–459.

Sullivan, A. P., and R. J. Weber (2006), Chemical characterization of the ambient organic aerosol soluble in water: 1. Isolation of hydrophobic and hydrophilic fractions with a XAD-8 resin, *J. Geophys. Res.*, *111*, D05314, doi:10.1029/2005JD006485.

Sullivan, A. P., R. J. Weber, A. L. Clements, J. R. Turner, M. S. Bae, and J. J. Schauer (2004), A method for on-line measurement of water-soluble organic carbon in ambient aerosol particles: Results from an urban site, *Geophys. Res. Lett.*, *31*, L13105, doi:10.1029/2004GL019681.

Takegawa, N., et al. (2005), Characterization of an Aerodyne aerosol mass spectrometer (AMS): Intercomparison with other aerosol instruments, *Aerosol Sci. Technol.*, *39*, 760–770.

Takegawa, N., T. Miyakawa, Y. Kondo, J. L. Jimenez, Q. Zhang, D. R. Worsnop, and M. Fukuda (2006), Seasonal and diurnal variations of submicron organic aerosol in Tokyo observed using the Aerodyne aerosol mass spectrometer, *J. Geophys. Res.*, *111*, D11206, doi:10.1029/2005JD006515.

Turpin, B. J., and H. J. Lim (2001), Species contributions to PM2.5 mass concentrations: Revisiting common assumptions for estimating organic mass, *Aerosol Sci. Technol.*, *35*, 602–610.

Warneck, P. (2003), In-cloud chemistry opens pathway to the formation of oxalic acid in the marine atmosphere, *Atmos. Environ.*, *26*, 2423–2427.

Weber, R. J., D. Orsini, Y. Daun, Y.-N. Lee, P. J. Klotz, and F. Brechtel (2001), A particle-into-liquid collector for rapid measurement of aerosol bulk chemical composition, *Aerosol Sci. Technol.*, *35*, 718–727.

Zhang, Q., M. R. Canagaratna, J. T. Jayne, D. R. Worsnop, and J.-L. Jimenez (2005a), Time- and size-resolved chemical composition of submicron particles in Pittsburgh: Implications for aerosol sources and processes, *J. Geophys. Res.*, *110*, D07S09, doi:10.1029/2004JD004649.

Zhang, Q., M. R. Alfarra, D. R. Worsnop, J. D. Allan, H. Coe, M. R. Canagaratna, and J. L. Jimenez (2005b), Deconvolution and quantification of hydrocarbon-like and oxygenated organic aerosols based on aerosol mass spectrometry, *Environ. Sci. Technol.*, *39*, 4938–4952, doi:10.1021/es0485681.

Zhang, Q., D. R. Worsnop, M. R. Canagaratna, and J.-L. Jimenez (2005c), Hydrocarbon-like and oxygenated organic aerosols in Pittsburgh: Insights into sources and processes of organic aerosols, *Atmos. Chem. Phys.*, *5*, 3289–3311.

J. L. Jimenez, Department of Chemistry and CIRES, University of Colorado, Boulder, CO 80309, USA. (jose.jimenez@colorado.edu)

Y. Kondo, T. Miyakawa, Y. Miyazaki, and N. Takegawa, Research Center for Advanced Science and Technology, University of Tokyo, 4-6-1 Komaba, Meguro-ku, Tokyo 153-8904, Japan. (y.kondo@atmos.rcast.u-tokyo.ac.jp; miyakawa@atmos.rcast.u-tokyo.ac.jp; yuzom@atmos.rcast.u-tokyo.ac.jp; takegawa@atmos.rcast.u-tokyo.ac.jp)

R. J. Weber, School of Earth and Atmospheric Sciences, Georgia Institute of Technology, Atlanta, GA 30332, USA. (rweber@eas.gatech.edu)

D. R. Worsnop, Aerodyne Research, Inc., Billerica, MA 01821-3976, USA. (worsnop@aerodyne.com)

Q. Zhang, Atmospheric Science Research Center, University at Albany, SUNY, Albany, NY 12203, USA. (qz@asrc.cestm.albany.edu)